J. Membrane Biol. 145, 21–31 (1995)

The Journal of
Membrane
Biology


# Responses of Neurons to Extreme Osmomechanical Stress

**X. Wan, J.A. Harris, C.E. Morris**
Neurosciences, Loeb Institute, Ottawa Civic Hospital, 1053 Carling Ave, Ottawa, Ontario, Canada K1Y 4E9

Received: 15 June 1994/Revised: 16 August 1994

**Abstract.** Neurons are often regarded as fragile cells, easily destroyed by mechanical and osmotic insult. The results presented here demonstrate that this perception needs revision. Using extreme osmotic swelling, we show that molluscan neurons are astonishingly robust. In distilled water, a heterogeneous population of *Lymnaea stagnalis* CNS neurons swelled to several times their initial volume, yet had a $ST_{50}$ (survival time for 50% of cells) >60 min. Cells that were initially bigger survived longer. On return to normal medium, survivors were able, over the next 24 hr, to rearborize.

Reversible membrane capacitance changes corresponding to about 0.7 $\mu F/cm^2$ of apparent surface area accompanied neuronal swelling and shrinking in hypo- and hyperosmotic solutions; reversible changes in cell surface area evidently contributed to the neurons' ability to accommodate hydrostatic pressures then recover. The reversible membrane area/capacitance changes were not dependent on extracellular $Ca^{2+}$.

Neurons were monitored for potassium currents during direct mechanical inflation and during osmotically driven inflation. The latter but not the former stimulus routinely elicited small potassium currents, suggesting that tension increases activate the currents only if additional disruption of the cortex has occurred.

Under stress in distilled water, a third of the neurons displayed a quite unexpected behavior: prolonged writhing of peripheral regions of the soma. This suggested that a plasma membrane-linked contractile machinery (presumably actomyosin) might contribute to the neurons' mechano-osmotic robustness by restricting water influx. Consistent with this possibility, 1 m*M* *N*-ethylmaleimide, which inhibits myosin ATPase, decreased the $ST_{50}$ to 18 min, rendered the survival time independent of initial size, and abolished writhing activity.

For neurons, active mechanical resistance of the submembranous cortex, along with the mechanical compliance supplied by insertion or eversion of membrane stores may account for the ability to withstand diverse mechanical stresses. Mechanical robustness such as that displayed here could be an asset during neuronal outgrowth or regeneration.

**Key words:** Osmotic shock — Capacitance — K conductance — Contractility — Volume — Blebs

## Introduction

Mechanical robustness and resilience are not commonly listed among the special hallmarks of neurons. Although neurons are dynamic tension-producing cells whose tenuous processes ramify in all directions and over long distances, they are often considered fragile. Were they indeed fragile, such structures would not persist; those processes embedded in tissues subject to mechanical changes (ranging from slow and sustained, as during embryogenesis, to abrupt and transient, as during muscle activity) would be especially vulnerable. How do neurons deal with mechanical stresses imposed from outside or stresses associated with their own outgrowth? Brute force, the approach used by plant cells with their exterior walls, is provided by cytoskeleton inside and by glia wrapping outside. But dynamic, mechanosensitive responses by the cell are probably more important in maintaining the potentially perilous morphology of neurons. At present, however, we know little about how cells monitor their mechanical status and respond accordingly (Watson, 1991; Morris, 1992; Wang, Butler & Ingber, 1993).

The unanticipated observations we report here challenged some of our own preconceptions about the fragility of neurons. We put cultured neurons in distilled water as a means of stretching their membranes and rupturing them quickly. Finding that rupture did not occur

*Correspondence to:* C.E. Morris

in tens of seconds or even a few minutes, we examined the cells' behavior more carefully. Two mechanical phenomena were noted—peripheral contractilelike activity and substantial increases in the apparent plasma membrane area. It is conceivable that both phenomena contribute to the ability of these cells to survive the hydrostatic pressure associated with extreme osmotic stress. Because neurons do not have to deal, in vivo, with extreme osmotic excursions, it is likely their robustness is not a reflection of special osmoregulatory prowess. Rather, their mechanical robustness is probably a broadly adaptive trait that facilitates the rapid and extensive morphological plasticity characteristic of neurons.

## Materials and Methods

### Cells and Solutions

Circumoesophageal ganglia were dissected from mature *L. stagnalis* and placed into an isotonic physiological solution, NS (*see* Table), and gently agitated with 0.25% type XIV protease (Sigma, St. Louis, MO) for 30 min. After the digestion period, the cells were washed with NS and plated in NS in Falcon 35 mm culture dishes by teasing apart the ganglia, thus releasing cells into the dish. All experiments were carried out at room temperature (20°C) 24–72 hours after the cells were plated.

Note that this procedure yields a heterogeneous population of unidentified neurons, and that no special substrates or growth factors were provided. By 24 hr in culture, the neurons had a broad range of morphologies, from heavily arborized, through fried egglike to round with little evident peripheral lamella. The last category of cells were chiefly used in these experiments; exceptions are noted.

Deionized double distilled water was used wherever there is a reference to distilled water (DW). The osmolarity of all solutions was measured with the Advanced MicroOsmometer (model 3MO).

Solution exchanges were made by hand using a Pasteur pipette; NS was drawn from the culture dish and replaced with experimental fluid. An exchange was done two more times. The whole procedure took <30 sec. Aliquots from the bottom of the dish were used in osmolarity measurements. When the experimental fluid was DW, the final osmolarity was 2.5 ± 2.0 mosm, $n = 9$ (SD).

### Viewing Cells

Observations were made using an Olympus IMT-2 microscope fitted with a Hoffman modulation contrast optics (objectives 10×, 20×, 40×). Video recordings were made with a Sony CCD video camera using JVC S-Xg video cassettes and a JVC BR-S601 MU super VHS or a time lapse JVC BR-905 OU recorder. Video images were made with a Sony UP-850 video graphics printer. Measurements were made either directly from these prints or from acetate traces from the video screen.

### Electrophysiology

Unarborized neurons with initial diameters of ~25–60 μm were used in conjunction with whole-cell and perforated patch recording techniques as described previously (Morris & Horn, 1991). Membrane conductance was studied using a ramp clamp protocol. Salines (Table) were designed so that $E_K$ would be in the −30 mV range. Osmotic perturbations were achieved by withdrawing or adding sucrose, so that in the bath solution, cells experienced no ionic perturbations. As cells swelled (or shrank), dilution (or concentration) of cell contents would have caused small depolarizing (or hyperpolarizing shifts) in $E_K$. Voltage clamp steps or ramps were used, as indicated. As before (Morris & Horn, 1991), the ramp protocol was designed (a) to avoid the voltage region that stimulates delayed rectifier $K^+$ channel activity, (b) to inactivate $I_a$ type $K^+$ channels and (c) to yield both directly measurable reversal potentials (i.e., currents either side of $E_K$) plus currents near the expected resting potential of the neurons.

Membrane capacitance was determined by integrating the capacitative current (yielding charge, in coulombs) associated with the downstep of a 25 msec 10 mV depolarizing pulse, i.e., down to the holding potential of −60 mV. The leak component of the current was excluded. Capacitance was calculated as the charge divided by 10 mV. Cell diameter was determined throughout the course of the experiment, either by direct observation (using an eyepiece micrometer) or subsequently from video recordings made via the attached CCD camera. Approximate cell area was calculated from the diameter by assuming that the cell was a sphere. Solution changes were achieved by bath perfusion. Experiments were carried out at room temperature.

## Results

### Time Course for Bursting in Distilled Water

Although some *Lymnaea* cultured neurons swelled and burst within 5 min of switching from normal saline (NS) to distilled water (DW), this was not the rule; neurons in DW typically swelled to bursting far more slowly. Nevertheless, the fact that some neurons swelled and burst within minutes suggests that the water permeability of cultured snail neurons was not preternaturally low. Some arborized neurons maintained their general form as they swelled. Others drew in their neurites into the rounding-up cell body. The histogram in Fig. 1*A* gives the time to burst for 28 individually monitored neurons of all sizes and shapes (arborized or not). About half the population of neurons did not burst by 1 hr (Fig. 1*A*) and some survived for 2 hr. The same was true for a population of unarborized neurons; the burst or survival time for 50% of the cells ($ST_{50}$) was 62 min, as shown in Fig. 1*B*. Typically, cells, when they ruptured, burst in a manner that suggested they were under pressure. Since this pressure had not been fully dissipated by cell swelling, the neuronal membrane cortex was evidently able to sustain nonzero pressures over many tens of minutes.

### Extent of Swelling

In a subset of neurons which (a) survived ⩾60 min and (b) were sufficiently round to allow volume estimates from average diameter, the time course of swelling in DW was followed (Fig. 1*C*). Relative volume increased monotonically, doubling in about 10 min. As was the case for *Lymnaea* neurons subjected to 0.3× normal saline (Morris, Williams & Sigurdson, 1989) rather than DW, there was no indication of volume regulatory de-

**Table.** Cells and solutions

| Bath solutions: Name | Normal physiological saline "NS" | Iso-osmotic "15K-iso" | Hypo-osmotic "15K-hypo" | Hyperosmotic "15K-hyper" | SubμM $Ca^{2+}$ | Elevated $K^+$ |
|---|---|---|---|---|---|---|
| NaCl | 50 | 0 | 0 | 0 | 0 | 34.5 |
| $CaCl_2$ | 3.5 | 3.5 | 3.5 | 3.5 | 0 | 3.5 |
| KCl | 1.6 | 15.5 | 15.5 | 15.5 | 15.5 | 17.6 |
| $MgCl_2$ | 2 | 2 | 2 | 2 | 5.5 | 2 |
| Glucose | 5 | 5 | 5 | 5 | 5 | 5 |
| HEPES | 5 | 5 | 5 | 5 | 5 | 5 |
| EGTA | 0 | 0 | 0 | 0 | 0.1 | 0 |
| Sucrose | 0 | 72 | 0 | 144 | 72,0,114* | 0 |
| Osmolarity | 110 | 120 | 53 | 216 | | |

| Pipette solutions: | Whole-cell (mM) | Perforated patch (mM) |
|---|---|---|
| KCl | 60 | 20 |
| $K_2SO_4$ | 0 | 35 |
| $CaCl_2$ | 0.2 | 0 |
| $MgCl_2$ | 2 | 2 |
| HEPES | 5 | 5 |
| EGTA | 2.2 | 0 |
| ATP.Mg | 5 | 0 |

* Sucrose was varied to set the osmolarity.
For the perforated patch experiments, 135 μg/ml of nystatin was added to the pipette solution.

crease. By 60 min, cell volume increased ~5-fold, entailing an approximately 3-fold area increase. Lipid bilayers can expand by only 2–3% before rupture (Evans, Waugh & Melnick, 1976; Wolfe, Dowgert & Steponkus, 1985); a 300% area increase clearly cannot be accounted for by elastic expansion. Recruitment of invaginated membrane and/or insertion of internal membrane stores to the plasma membrane must have occurred, an issue that is explored below by capacitance measurements.

### Effect of Cell Size on Burst Time

The time that it takes a cell to burst in DW reflects its strength and general ability to protect its plasma membrane from lytic tension. Figure 1*D* shows that, in the heterogeneous population of neurons, cells of larger initial size survived longer, with a linear correlation between burst time and diameter. No specific physical meaning is attributed to the regression, but its positive slope directly contradicts expectation for a cell with a soap bubblelike membrane. In such structures, strength is governed by surface tension according to Laplace's law ($T = Pd/4$, where $T$ is tension, $P$ is transmural pressure, $d$ is diameter). Neurons behaving strictly as Laplacian thin-walled spheres would have burst faster the larger the cell diameter. Because the plot indicates that plasma membrane tension was not routinely higher in larger cells, other factors must have over-ridden the Laplacian effect.

For a cell behaving as a simple osmometer, the rate of cytoplasmic dilution would increase as diameter decreased, making smallness unfavorable for survival. Since smaller cells were indeed more vulnerable, a more rapid dilution may explain their more rapid demise. However, given that cells survived as long as 2 hr in DW, it seems implausible that passive dilution rates alone accounted for the degree of protection enjoyed by cells. Other possible advantages of a large ratio of [cytoplasmic volume]:[surface area] need to be considered. In larger cells, each unit area of surface membrane under mechanical stress has available a greater cytoplasmic volume to contribute (a) fortifying cytoskeletal elements to retard swelling and (b) membrane reserves to prevent rupture as swelling proceeds.

### Survival During Reorganization of Processes and Plasma Membrane

Most arborized neurons exposed to DW became globular. Once under way, rounding up took several minutes and was particularly dramatic (a) in cells with extensive neurites (neurites often severed themselves from their

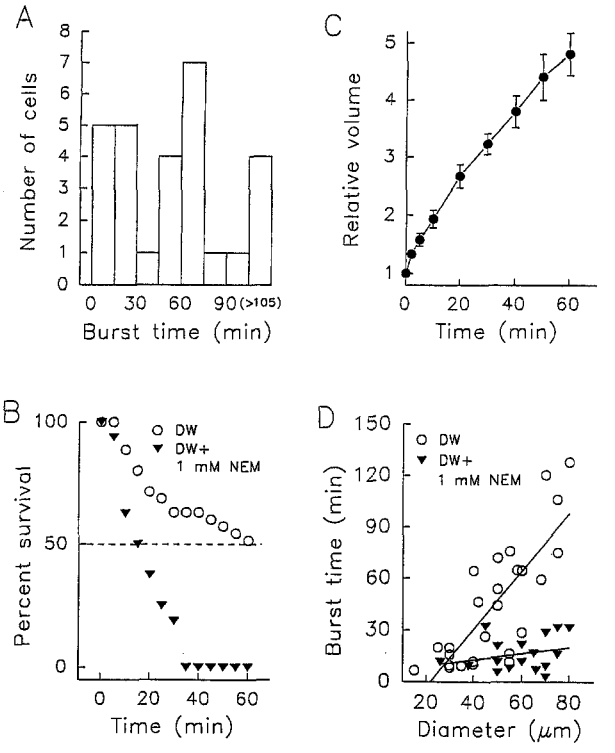


**Fig. 1.** Swelling and bursting. (*A*) Histogram of burst times in *DW* for an unselected population (i.e., variously arborized) of neurons. (*B*) Survival curves for neurons in *DW* (control) and in *DW + NEM*. Round unarborized neurons only were used for these experiments. Neurons were from six separate digests, with ganglia from two snails/digest. The percent survival, was 100% times the fraction of the population of monitored neurons monitored that had not burst at time *t;* the burst times were measured from time lapse recordings of single fields with 1–4 neurons/field. The broken horizontal line at 50% indicates $ST_{50}$s of 62 min and 18 min for control and *NEM* conditions. (*C*) Relative volume of cells swelling in *DW*. Data from five round neurons that survived ≥60 min and showed no writhing were used. Volumes doubled and quadrupled in about 10 and 45 min respectively. (*D*) Burst time *vs.* initial diameter of the neurons for the same cells as in *B*.

growth cones, resealing as they did so, and were retracted) and (b) in freshly isolated neuronal somata bearing intact axonal processes which, like neurites that had grown in culture, retracted in DW. Such observations signal that even in the face of extensive restructuring of cytoplasm and extensive rearrangement of plasma membrane (including resealing of severed neurites), neurons withstood considerable hydrostatic pressures without rupture. It can be assumed, therefore, that stable, long-range cytoskeletal anchoring arrangements are not what enable these neurons to withstand stretching forces. Dynamic structures associated with the plasma membrane and cortical cytoplasm must explain the neurons' mechanical resilience.

### Electrophysiological Correlates of Swelling

Cell swelling is not accompanied by a capacitance increase if swelling merely smooths out previously voltage clamp-accessible surface irregularities (e.g., Ross, Garber, & Cahalan, 1993). A capacitance increase would, however, result if deep cleft- or tubulelike invaginations became clamp accessible as a result of swelling. Likewise, a capacitance increase would result if swelling involved insertion of vesicular membrane stores into the plasma membrane. The two recording configurations we used differ in their impact on cytoplasmic integrity. Insofar as swelling entailed simple smoothing of previously clamped surface irregularities, the whole-cell configuration should be adequate, but perforated patch should more reliably demonstrate the extent of capacitance changes resulting from biochemically demanding processes (i.e., ones requiring intact cytoplasm). We recorded only from round neurons without neurites.

For both configurations, downshocks to 0.47× normal (15K-hypo) then upshocks to 1.7× normal (15K-hyper) were used (Table; these solution names indicate that external $[K^+]$, and hence the initial $E_K$ was fixed during osmolarity changes). Shocks were solely osmotic; sucrose was withdrawn or added and ions were not changed. Nystatin-perforated membrane constitutes a greater barrier to water movement than a patch-free pipette tip (as in whole cell). Thus, in perforated patch, even more than in whole cell, osmotic water fluxes should alter hydrostatic pressure. In practice, the extents and rates of swelling and shrinking were similar for the two configurations.

Once good perforated patch conditions had been established, capacitance of neurons was monitored for an additional 10–15 min to ensure a stable baseline. In twenty cells (whose average capacitance was 58 pF), the capacitance variation between the start and end of this period was only 0.4 ± 0.06 pF. The last measurement was used for comparisons during osmotic shock.

An upshock to 15K-hyper (rather than 1×, i.e., 15K-iso, the initial bathing solution) speeded shrinking, allowing us to obtain capacitance measurements over a wider range of cell diameter. Neurons were allowed to swell until they had measurably larger diameters and several size and capacitance measurements were made in 15K-hypo before neurons were switched to 15K-hyper; generally this involved ~20 min of swelling and ~30 min of shrinking.

### Whole-Cell Recording

The relationship between cell capacitance and apparent area measured under whole-cell clamp in the control solution (15K-iso) was 0.9 ± 0.2 $\mu F/cm^2$ (n = 6). For biological membranes, the direct relationship between capacitance and membrane area, as determined by Sokabe et al. (1991) is 0.7 $\mu F/cm^2$, so 0.9 $\mu F/cm^2$ is consistent with a somewhat irregular membrane under clamp in the resting cell. Moreover, substrate-adherent plasma membrane may have contributed less capacitative current.

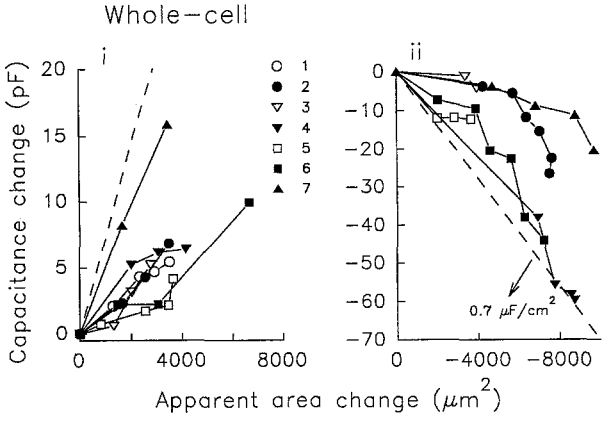


**Fig. 2.** Whole-cell recording configuration. Capacitance changes as a function of apparent area changes in neurons (each neuron is assigned a different symbol) as they swelled (*i*) and, subsequently, shrank (*ii*). The solutions and recording conditions used are detailed in the text. Broken lines correspond to 0.7 $\mu F/cm^2$. Symbols for cells 1–7 are indicated. Cell 1 ruptured, and so is not represented in the shrinking data.

The outcomes of the whole-cell experiments are given in Fig. 2. To put the swelling/capacitance and shrinking/capacitance results in perspective, a line corresponding to 0.7 $\mu F/cm^2$ is plotted along with our data. In none of the seven cells tested did capacitance increase at the rate of 0.7 $\mu F/cm^2$ during swelling (Fig. 2*i*), but all showed a tendency to increase their capacitance as they swelled. When subsequently placed in shrinking solution (15K-hyper), six cells (cell 1 ruptured prior to shrinking) tended to decrease in capacitance and area, with one cell following close to the 0.7 $\mu m/cm^2$ line (Fig. 2*ii*).

Since we used a mixed population of neurosecretory, inter-, motor and sensory neurons, the observed variability in area/capacitance change measurements is probably, in part, cell-type dependent. Another possible source of variation is that the spherical, unarborized neurons used may have had variable amounts of small lamellae obscured by the cell body. In general, however, in neighboring arborized neurons exposed to the hypoosmotic salines, attachments were remarkably stable.

## Perforated Patch Recording

For neurons voltage-clamped in the perforated patch configuration and bathed in the same control solution as for whole cell experiments, the initial relationship between cell capacitance and apparent area was 1.3 ± 0.1 $\mu F/cm^2$ ($n$ = 18). When such cells ($n$ = 10) were subjected first to 15K-hypo and then to 15K-hyper, they too swelled and then shrank while exhibiting increases then decreases in capacitance (Fig. 3*Ai* and 3*Aii*, respectively). Although there was substantial cell-to-cell variability, the results for individual cells were about evenly dispersed on either side of the 0.7 $\mu F/cm^2$ line. This was the case during both swelling and shrinking.

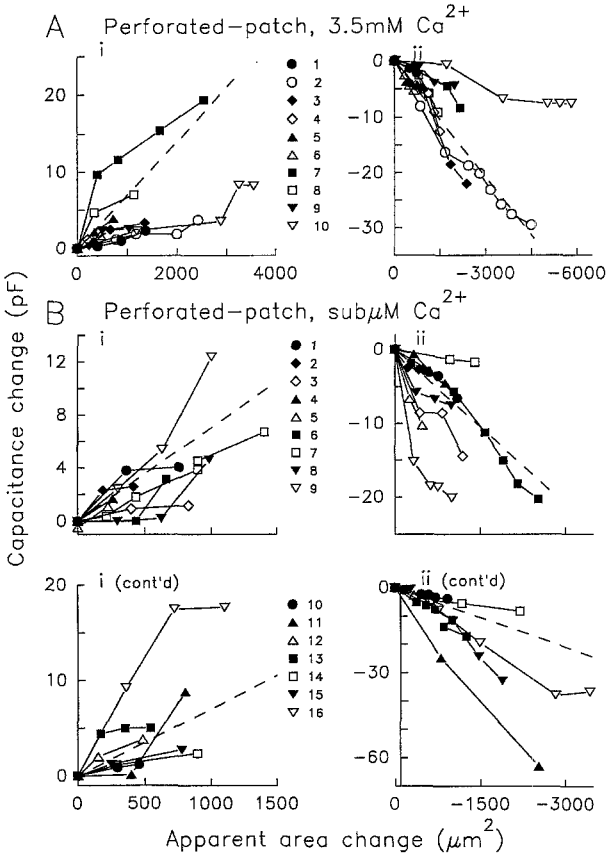


**Fig. 3.** Perforated patch recording configuration. Capacitance changes as a function of apparent area changes with normal extracellular [$Ca^{2+}$] (*A*) and with submicromolar $Ca^{2+}$ (*B*) in the bath as neurons swelled (*i*) and, subsequently, shrank (*ii*). In part (*B*), data from 16 cells are spread over two sets of graphs for visibility. Note the scale changes in the ordinate. The solutions and recording conditions are detailed in the text. Broken lines correspond to 0.7 $\mu F/cm^2$.

In the perforated patch experiments it was noted anecdotally that vacuolelike dilations (as observed by Reuzeau et al., 1995) formed at the base of the cells during the shrinking phase in 15K-hyper. As they were below the focal plane used to monitor cell diameter and it is impractical to adjust focus while recording, the extent of membrane associated with the dilations could not be gauged.

## Capacitance Changes in Sub-micromolar Extracellular $Ca^{2+}$

The perforated patch experiments were repeated using 15K-hypo and 15K-hyper with sub-μmolar $Ca^{2+}$ (Fig. 3*Bi* and 3*Bii; see* Table 1) and elevated $Mg^{2+}$. These solutions would have largely eliminated exocytosis that

required an influx of extracellular $Ca^{2+}$, though they would not, of course, have prevented release of $Ca^{2+}$ from intracellular stores. In the sub-μmolar $Ca^{2+}$ isomotic control solution (with 72 m*M* sucrose) for these experiments, the initial relationship between cell capacitance and apparent area was $1.0 \pm 0.1$ μF/cm$^2$ ($n = 16$), not significantly different from the apparent specific capacitances with $Ca^{2+}$ (perforated patch or whole cell). As in the normal $Ca^{2+}$ experiments, swelling and shrinking occurred in the hypo and hyper solutions. And as in normal $Ca^{2+}$, capacitance tended to increase during swelling and to decrease during subsequent shrinking. The responses again covered a wide range, but, in spite of the variability, they fell about evenly on either side of the 0.7 μF/cm$^2$ line.

### Conductance Changes During Direct Inflation and Osmomechanical Inflation

In the above experiments, neurons were subjected to osmomechanical perturbations, but only capacitance, not ionic current, was monitored. Efflux of ions through channels is, however, a common cellular mechanism for relief of osmotic swelling stress. Although *Lymnaea* neurons have $K^+$-selective stretch channels (Morris & Sigurdson, 1989), inflation of the neurons under whole-cell clamp was found to be at best a poor stimulus for them (Morris & Horn, 1991). To provide a better picture of the cellular response to the perturbations that yielded capacitance changes, we also monitored conductances under a variety of conditions.

Using a larger sample size than previously, we retested the effect of direct positive pressure on $K^+$ selective currents (Fig. 4*A,B*). As before, we noted that at pressures just above 10 mm Hg applied through the pipette, neurons inflated rapidly and ruptured. At pipette tips, patches of membrane from the same cells withstand suction of as much as 200 mm Hg, so the lower pressure-tolerance of whole neurons may reflect a Laplace Law effect associated with greater radius of curvature. Nine cells were tested by comparing ramp *I-V* curves obtained without pressure and then during a sustained pressure (5–11 mm Hg). Pressure was increased 1–2 mm Hg between ramps until the neuron ruptured. For seven of the cells, voltage-step protocols were used prior to the first pressure application, yielding families of voltage-dependent $K^+$ currents; samples of the resulting *I-V* relations are given in Fig. 4*C*. This demonstrated that the cells were adequately clamped and also provided a measure of the reversal potential for a $K^+$-selective current in the solutions used to detect mechanosensitive $K^+$ currents (Elevated $K^+$ in the bath, whole-cell solution in the pipette; *see* Table). The predicted $E_K$ was −31 mV. The voltage-dependent currents measured at steady state (from $I_a$ type $K^+$ channels; *see* Morris & Horn, 1991) reversed at $-28 \pm 3$ mV ($n = 7$).

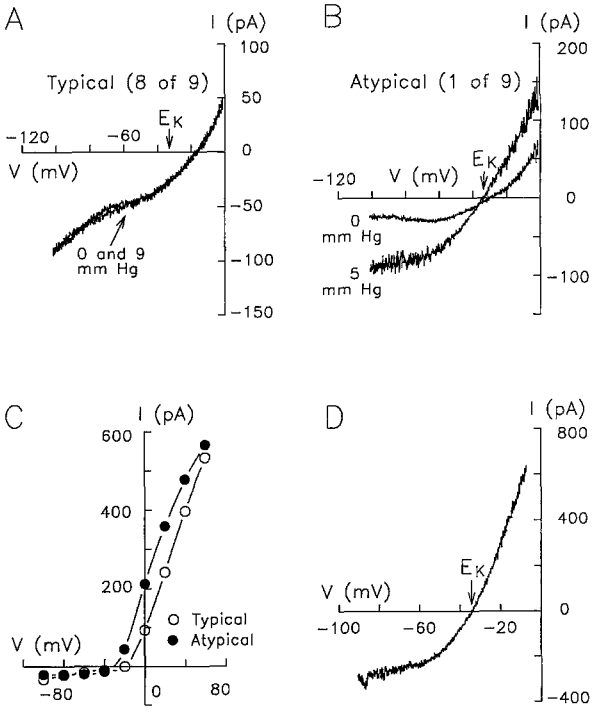


**Fig. 4.** Current-voltage relations. Conductive properties of inflated and osmotically swollen neurons. (*A–C*) Whole-cell clamp configuration. In (*A*) and (*B*), a ramp protocol (*see* Materials and Methods) was used and inflating pressure was applied via the recording pipette. In (*C*), voltage steps were used to elicit voltage-activated $K^+$ currents; the curve labeled typical is for the neuron whose lack of mechanosensitive currents is illustrated in (*A*), and that labeled atypical is for the neuron that exhibited the mechanosensitive current in (*B*). (*D*) Perforated patch clamp configuration. An example of a difference current (ramp data during swelling minus that before swelling) in an osmotically swollen neuron whose capacitance was also monitored (*see* text for details).

In eight of nine cells, pressure had induced no new current at the last measurement obtained before the cell ruptured, as illustrated by the graph labeled "*Typical*" in Fig. 4*A*. In only one cell (*see* graph labeled "*Atypical*" in Fig. 4*B*) did the applied pressure induce a current. The difference current reversed in the vicinity of $E_K$, and so may have flowed through stretch-activated $K^+$ channels. The cell ruptured seconds after the pressure-induced member of the illustrated pair of currents was obtained, indicating that the current was induced by a near-lytic tension.

Examined at the single-channel level, *Lymnaea* neurons invariably exhibit stretch-activated (SA) K channels (Morris & Horn, 1991). But examined macroscopically during positive pressures meant to mimic the hydrostatic pressure that drives osmotic swelling, most neurons yielded no mechanosensitive $K^+$ currents. This confirms our earlier conclusion that increased membrane tension alone is not usually an adequate stimulus for these neuronal "stretch-activated" $K^+$ channels *in situ*.

Ionic currents were, however, induced when neuro-

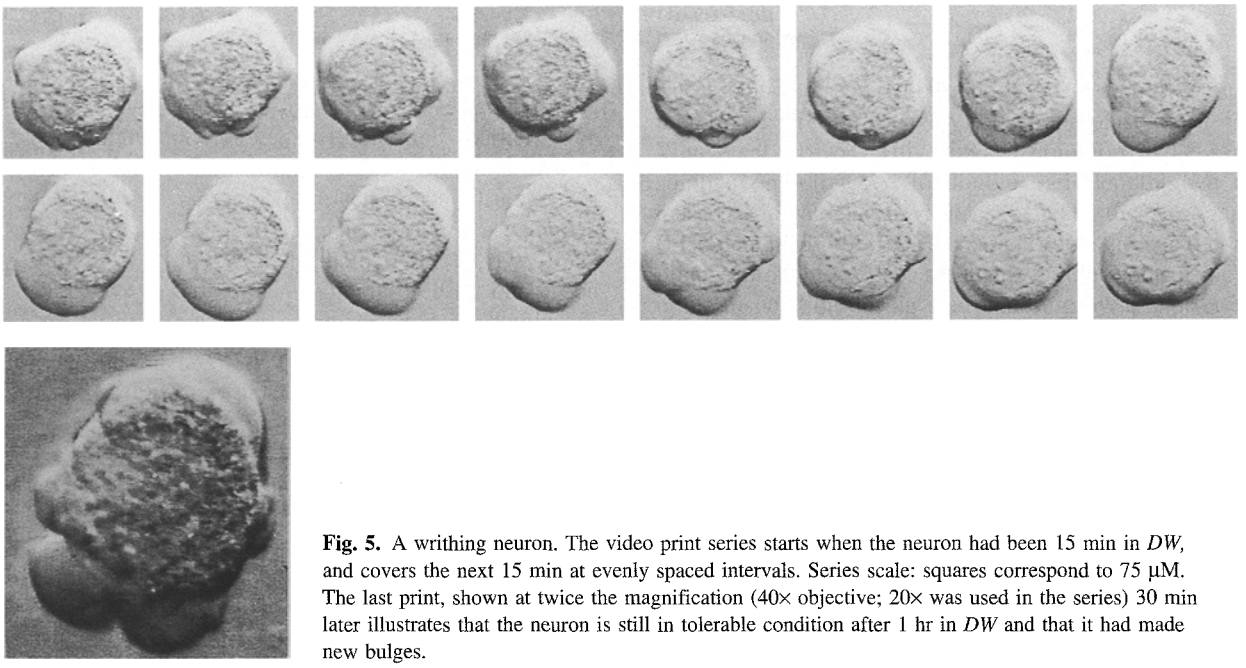

**Fig. 5.** A writhing neuron. The video print series starts when the neuron had been 15 min in *DW*, and covers the next 15 min at evenly spaced intervals. Series scale: squares correspond to 75 μM. The last print, shown at twice the magnification (40× objective; 20× was used in the series) 30 min later illustrates that the neuron is still in tolerable condition after 1 hr in *DW* and that it had made new bulges.

nal cell bodies swelled osmotically in 15K-hypo. This is in contradiction to our findings for isolated swollen growth cones (Morris & Horn, 1991). In five swelling neurons, we alternately applied voltage ramps to monitor currents around $E_K$, and small steps to monitor capacitance (*as above*). New current was elicited by swelling; the reversal potential of the difference currents (Fig. 4*D*) was −36 ± 2 mV ($n$ = 5), close to $E_K$. The apparent current density (at −60 mV) of this difference current was 0.065 ± 0.02 pA/μm$^2$, corresponding to either 9.2 pA/pF (measuring swollen cell diameter and assuming 0.7 μF/cm$^2$) or 20 ± 7 pA/pF (referring the current to the directly measured capacitance of swollen cells). If the 0.065 pA/μm$^2$ was carried by SA K channels at a density of 1/μm$^2$ and passing 1 pA at −60 mV (*see* Morris & Horn, 1991) the single-channel open probability would be 0.065.

There are no specific blockers for SA K channels which could be used to establish whether the swelling induced $K^+$ current was carried by SA K channels. In single channel studies, however, SA K channels can be distinguished from many other $K^+$ channels, including $K_{Ca}$, by their insensitivity to 1 m*M* extracellular TEA (Small & Morris, 1995). We therefore asked whether 1 m*M* TEA in the bath abolished the swelling-induced $K^+$ conductance. Ramp *I-V* data obtained with and without TEA in neurons swollen in 15K-hypo indicated no TEA sensitivity. Swelling induced difference currents reversed at −31 ± 3 mV ($n$ = 14) for control and at −30 ± 4 mV (n = 8) for TEA exposure and the current magnitude at −60 mV was not detectably affected (14 ± 4 pA and 12 ± 4 pA respectively). Thus, $K^+$ ions may have used SA K channels, but mechanism of $K^+$ conductance increase is unresolved. Activation of $K^+$ channels present prior to swelling (with either stretch or altered cytoplasmic chemistry leading to activation) and recruitment of new membrane bearing active $K^+$ channels could both have contributed.

### Writhing Contractile Behavior

For round neurons exposed to DW, reorientation movements occurred when swelling disrupted adhesions to the substrate. But in addition to these brief recoil actions, a strikingly different, protracted cellular behavior was noted in some cells: movements of the periphery that, especially as viewed by time-lapse, would aptly be described as contractile writhing. In writhing neurons, bulges periodically ballooned out alarmingly (the cells seemed about to explode) only to be retracted over the next minutes (Fig. 5). Bulging-then-retracting areas generally corresponded to areas of relatively clear-looking cytoplasm, as if writhing did not require uninterrupted granular cytoplasm between the cortex and perinuclear region.

In neurons, writhing (defined operationally as a cycle of bulge/retraction occurring twice or more in at least one region) was observed in 8 of 23 unarborized cells monitored over about 60 min in DW. Some cells exhibited a single bulge/retraction cycle; since these might conceivably have resulted from a complex passive recoil the cells were scored as nonwrithers. A contractile restorative force would, however, be required for the repeated bulge/retraction cycles that we scored as writhing. By this conservative definition, contractility during osmotic stress was evident in >⅓ of the neurons.

### The Viability of Osmotically Stressed Neurons

To do contractile work, cells must be sufficiently healthy to fuel molecular motors and to control intracellular ions within reasonable limits. If writhing, seen in neurons even after an hour of the ultimate osmotic insult, indeed represented contractile work, the cells must have been physiologically viable. To further confirm that the DW survivors were not merely nonruptured membrane bags, but alive and well, we returned them to growth medium and checked them 24 hr later. Neurons from two enzymic digests (two animals per digest) were used; from each, two dishes of neurons plated the previous day were exposed 2 hr to DW. Within minutes of return to growth medium, neurons became extensively vacuolated; this was a universal and transient post-swelling response (*see* Reuzeau et al., 1995). Additional assays were not required to conclude that the bloated, mis-shapen DW survivors must indeed have been alive, since, 24 hr later, neuronal somata had reassumed their granular compact appearance and many neurons showed extensive rearborizations. Individual neurons were not monitored, but, because prolonged DW exposure causes neurons to retract or sever their processes, arborizations seen at 24 hr must have represented *de novo* outgrowth from newly organized growth cones.

### Effects of N-ethylmaleimide (NEM)

Although the writhing seen under hydrostatic pressure suggests that neuronal cortex has contractile abilities, contractile work may or may not retard cell swelling. If cortical squeezing effectively countered hydrostatic pressure, cells would rupture sooner in DW when myosin is inhibited. Specific mysosin reagents are not available; the anticontractility agent we used, NEM, is a nonspecific sulfydryl reagent with, among its many cellular actions, a pronounced antimyosin ATPase activity. NEM applied to nonmuscle cells in culture demonstrably disrupts mysosin structure (Karlsson & Lindberg, 1985; Lawson, 1987). We looked at three aspects of cell function in NEM-treated cells under osmotic stress: $ST_{50}$, writhing and dependence of burst time on initial size. In initial tests, 1 m*M* NEM was applied for 60 min in NS; in the absence of a hypo-osmotic shock, NEM did not induce detectable swelling or cell shape changes.

Fig. 1*B* compares survival curves and $ST_{50}$ (the survival time for 50% of the cells) for unarborized cells in DW without NEM and with 1 m*M* NEM. NEM markedly reduced the ability of the cells to tolerate the severe swelling stress. Whereas $ST_{50}$ was 62 min without NEM, it fell to 18 min with NEM. As Fig. 1*D* shows, NEM also abolished the dependence of burst time on the initial cell size. Pursuing the earlier argument to the effect that larger cells might overcome Laplace Law effects via their lower surface/volume ratio, it follows that the loss of the cell-size trend in NEM would represent a shift (albeit incomplete) toward governance by Laplace's Law. One possibility, therefore is that NEM reduced protective actions (e.g., cortical contractility, recruitment of membrane reserves) provided by the cytoplasm underlying the stressed plasma membrane.

Finally, we monitored, over a period of at least 1 hr, 26 unarborized cells in 1 m*M* NEM/DW and watched for writhing. Of 26 neurons, 9 blebbed, that is, formed readily visible protrusions prior to bursting, but the blebs were never retracted. This swelling behavior was not writhing, as defined above; writhing was not seen in any of the 26 NEM-treated cells.

## Discussion

### Osmomechanical Robustness

Conventional wisdom has it that animal cells exposed to distilled water (DW) rupture almost immediately. Apart from being ensconced *in situ* in a restraining ganglionic sheath, the snail neurons we used are not specialized for dealing with acute osmotic stress (Morris, Williams & Sigurdson, 1989). Yet, unprotected in culture, they managed to survive prolonged exposure to DW. The conventional wisdom, based largely on erythrocytes, is perhaps misleading. Erythrocytes lack cytoplasmic membrane reserves, yet mobilization of membrane reserves may play a key role in the osmomechanical resilience of animal cells.

Neurons may be resilient enough to survive extreme hyposmotic stress because they have abundant cellular machinery for performing a task not uncommon among animal cells—i.e., rapid shape change. Other examples, drawn from vertebrate cells, of resilience under osmotic stress, suggest that this notion is worth exploring. Avian sympathetic neurons exposed to 50% dilution not only survive but arborize robustly (Bray et al., 1991). Mammalian cardiac cells in 50% saline show evidence of generating a mechanical force that counters the solution's swelling-induced stress (Suleymanian & Baumgarten, 1994). Neutrophil volume can increase 8-fold without rupture (Stoddard, Steinbach & Simchowitz, 1993), a point that may be relevant to the fact that white blood cells characteristically survive hyposmotic shocks used clinically to rupture erythrocytes. Since *Lymnaea* neurons under extreme hyposmotic stress writhed, it is interesting that human T-lymphocytes in 50% saline writhe by repeatedly extending and retracting "uropods" (L. Schlichter, *personal communication*). The morphology of swelling Ehrlich ascites cells suggests that they do the same, though motions of individual cells were not followed (Wilkerson, DiBona & Schafer,

1986). Neuronal processes, cardiac cells and circulating white cells, are all exposed to substantial mechanical stresses on a regular basis. Epithelial cells that deal with both mechanical and osmotic perturbations might be the toughest of all; not surprisingly, bladder epithelial cells make rapid reversible area/capacitance adjustments to their plasma membrane in response to either mechanical or osmotic stretch (Lewis & de Moura, 1982).

We postulate that the toughness of *Lymnaea* neurons, rather than being bizarre, represents an enhanced version of a mechanical robustness inherent in membrane-rich, morphologically dynamic cells. Given that bigger *Lymnaea* neurons survived longer in DW, the large size of *Lymnaea* neurons compared to most vertebrate cells may be instrumental in their relative toughness. In addition, the low osmotic strength *Lymnaea* blood (about half that of mammalian blood) would preadjust their neurons to a reduced osmoticum; we found that equally large neurons (bag cells) of the marine mollusc, *Aplysia,* could withstand exposure to 10% saline but not to DW (*see* Reuzeau et al., 1995).

Speculating on possible scenarios by which cytoskeleton could actively counter osmotic swelling, Mills (1987) noted the difficulty in nonmuscle cells of obtaining evidence for contractile responses. The typical rounding-up motions of swelling cells may obscure any cortical squeezing contractions. Nevertheless, contractile actions which retarded rounding (i.e., promoted irregularity) should be advantageous. Were a cell a true thin-walled sphere, it could tolerate no shape change without rupture of its essentially inelastic bilayer. By contrast, irregular cells can assume a continuum of shapes of fixed surface area/volume ratio. Because the strength of thin shells increases with curvature, cells with irregularities would also be tougher than perfectly smooth ones. Irregularities of high curvature (invaginations, microvilli) also augment membrane area for osmolyte transporters. Thus even if cortical contractile elements did not directly expel cell water from swelling cells, their activity could enhance mechanical robustness in cells simply by favoring cellular irregularity and corrugations of surface membrane.

If the simple mechanical strength of membrane/cortex is instrumental in retarding water influx as hydrostatic pressure develops, it becomes interesting to consider the possibility that net water influx promotes hydration-sensitive conformation changes (e.g., Colombo, Rau & Parsegian, 1992; Suzuki, Yamazaki & Ito, 1989) of cortical cytoskeleton proteins that enhance cortical strength and/or increase membrane microroughness (*see* Schmidt et al., 1993).

An analogy for the neuronal writhing that we observed in hypo-osmotically stressed neurons might be: a tethered, slowly inflating balloon in whose wall is embedded a contractile mesh. If mesh contractions are isotropic, the balloon does not writhe. The rate of inflation depends on the relative magnitudes of contractile and inflation pressures. If contractile intensity fluctuates so that contractions are globally anisotropic, aneurisms form then retract with the shifting contractile forces—the balloon writhes. If, in addition, the balloon contains several smaller balloons (analogous to the nucleus and adherent perinuclear cytoplasm and to any large osmotically swollen vacuoles), these are pushed about by the peripheral contractions, causing bulges to advance then retract in a somewhat abrupt manner. It will be helpful to monitor writhing cells by confocal microscopy; a preliminary observation (L. Mills and C. Morris) using a membrane dye revealed that large vacuoles can form in the upper hemisphere of osmotically swollen neurons. The nonwrithers in our experiments (15 of 23 cells) did not necessarily lack contractile activity; as suggested by the balloon analogy, their contractility may simply have been more nearly isotropic.

Bleb formation during osmotic swelling and various other regimes that disrupt the integrity of the cortical cytoskeleton has been widely reported (e.g., Gabai & Kabakov, 1993; Jurkowitz-Alexander et al., 1992). Writhing such as we observed in *Lymnaea* neurons may be a manifestation of the blebbing phenomenon under conditions in which the cell is still able to mount a partially effective counterforce.

### Membrane Capacitance, Membrane Currents and Osmomechanical Stress

Where antiswelling measures fail to counter peripheral tension, a cell must either rupture or inflate. In principle cortical tension could act as a direct signal to trigger recruitment of the additional plasma membrane needed to prevent rupture.

We used osmotic pressure to increase membrane tension, but it is a problematic stimulus, since its mechanical and chemical components are not readily separated. We found that osmotic swelling and shrinking were associated with capacitance increases and decreases but are uncertain whether cortical tension changes were the trigger for these adjustments. Ideally, the mechanical component of osmotic swelling could be mimicked by inflating the cell with positive pressure in the whole-cell configuration. We found, however, that swelling was almost undetectable except suddenly as the cell exploded.

Pressures just below those causing membrane rupture induced $K^+$ channel activity (presumably SA K channels) in only 1 of 9 cells; 2 of 4 cells gave small responses in earlier trials (Morris & Horn, 1991). We recently demonstrated by single-channel recording that *Lymnaea* neuron SA K channels become more stretch-sensitive following mechanical disruption of the membrane/cortex or after cytochalasin D treatment (Small & Morris, 1994). This suggests that in about one experiment in four (i.e., $(1 + 2)/(9 + 4)$), the inflating pressure

may have disrupted cortical cytoskeleton prior to rupturing the membrane, allowing tension to act on the channel-bearing bilayer.

Likewise, because we can not inflate neurons in a controlled manner using positive pressure, we can not gauge the direct effect of cortical tension on plasma membrane area. Presently, we can say that capacitance changes are associated with swelling and shrinking, that they are more pronounced when the cytoplasm is least perturbed chemically, that they can occur without an influx of extracellular $Ca^{2+}$, and that they can occur (under whole cell clamp) with the $Ca^{2+}$ chelator, EGTA, in the pipette. Direct determinations of cytoplasmic $Ca^{2+}$ will be needed to establish whether the changes are $Ca^{2+}$-independent. Nevertheless, an interesting possibility is that membrane tension directly controls rates of insertion and/or retrieval of membrane stores at the cell surface. A possible precedent for direct tension-control of membrane disposition is seen in the ameboid contractile vacuole (Heuser, Zhu & Clarke, 1993).

The swelling associated capacitance and $K^+$ current increases suggest that one avenue neurons use to avoid mechano-osmotic rupture is recruitment of channel-bearing membrane from cytoplasmic reserves. Neural membranes are under tension during growth (*see* Bray, 1992; Lamoureux et al, 1989); for a growing neuron, an ability to increase membrane area according to cell tension could both prevent rupture and foster outgrowth. In nongrowing cells, area increase in response to stretch would be an emergency measure to prevent rupture, but subsequent area reduction would be needed when the stress was removed. For minor stretching or swelling forces, it might be simpler to resist cell shape changes by countering the stress, thus preserving cell volume, cell osmolytes and cell area in a single stroke. Subsurface contractile machinery—machinery involving proteins that should be sensitive to NEM—might serve in this capacity. In the extreme conditions we used, NEM increased the fragility of neurons and abolished their contractile writhing. The tantalizing possibility that actomyosin contractility is implicated in these two NEM effects, and hence in more subtle cell responses to swelling and stretch, will require further investigation when specific reagents are available; NEM acts on a multitude of sulfhydryl containing proteins, so the effects observed here can only be regarded as consistent with the possibility of motor protein involvement.

### Comparison with a Less Robust *Lymnaea* Cell

*Lymnaea* heart cells have been subjected to DW in a different experimental context (Morris & Moore, 1992). The pattern of efflux of $^{86}Rb^+$ from these cells indicated that they did not lyse immediately. Nonetheless, heart cells are considerably more fragile than neurons; 50% of the heart cells survived ~12 min and the rest lysed by ~40 min though they were protected by basement membrane. Cultured heart cells lacking basement membrane lysed in ~1 min when exposed to 0.2× normal saline (Morris, Williams & Sigurdson, 1989). Neurons in DW, by comparison, had an $ST_{50}$ of >60 min. Why should neurons be more robust than heart cells from the same organism? The answer may relate to the fact that neurons possess the wherewithal to create extensively arborized shapes and to continually modify these shapes according to the demands of tissues in which their processes are embedded. As we showed, neurons can reversibly alter their membrane area when they are subjected to tension changes; this would facilitate neuronal remodelling. *In situ,* it is inevitable that tension vectors in branches of an arborized neuron would be highly localized. The machinery that allows neurons to respond quickly to locally diverse tension changes by locally changing their membrane area should render them robust in the face of a general tension increase. Other cells types which adjust their morphology to the prevailing mechanical load include fibroblasts and bladder epithelium, and both can evidently reversibly adjust cell shape and membrane area in response to stretch/release stimuli (Sukhorukov, Arnold & Zimmermann, 1993; Lewis & de Moura, 1982).

### How Does Area Increase and Decrease?

Is fusion of vesicular membrane stores, unfolding of invaginated membrane or a combination of both responsible for capacitance increases in swelling cells? We do not yet know. However the changes are achieved, it is remarkable that despite prevailing hydrostatic pressure and the disrupted, diluted state of the cytoplasm of a DW-exposed neuron, regions of new and of original membrane (bilayer plus cortical cytoskeleton) mesh together and continue to resist rupture.

Some form of mechanosensitive membrane trafficking may be involved in the capacitance increases and decreases. Membrane trafficking would, by definition, be considered mechanosensitive (a) if taut membrane incorporated new membrane at a higher rate than slack membrane and/or (b) if slack membrane exhibited higher rates of retrieval from the surface to internal stores than taut membrane. Mechanosensitive control of membrane disposition, whatever the mechanism, could potentially explain both reversible VLD (vacuolelike dilation) formation (Reuzeau et al., 1995) and the reversible capacitance changes observed here.

This work was supported by a NSERC Canada research grant to CEM.

## References

Bray, D., Money, N.P., Harold, F.M., Bamburg, J.R. 1991. Responses of growth cones to changes in osmolality of the surrounding medium. *J. Cell Science* **98**:507–515

Colombo, M.F., Rau, D.C., Parsegian, V.A. 1993. Protein solvation in allosteric regulation: a water effect on hemoglobin. *Science* **259:** 1335–1336

Evans, E.A., Waugh, R., Melnik, L. 1976. Elastic area compressibility modulus of red cell membranes. *Biophys. J.* **16:**585–595

Gabai, V.L., Kabakov, A.E. 1993. Tumor cell resistance to energy deprivation and hyperthermia can be determined by the actin skeleton stability. *Cancer Letters* **70:**25–31

Heuser, J., Zhu, Q., Clarke, M. 1993. Proton pumps populate the contractile vacuoles of *Dictyostelium amoebae*. *J. Cell Biol.* **121:**1311–1327

Jurkowitz-Alexander, M.S., Altschuld, R.A., Hohl, C.M., Johnson, J.D., McDonald, J.S., Simmons, T.D., Horrocks, L.A. 1992. Cell swelling, blebbing and death are dependent on ATP depletion and independent of calcium during chemical hypoxia in a glial cell line (ROC-1). *J. Neurochem.* **59:**344–352

Karlsson, R., Lindberg, U. 1985. Changes in the organization of actin and myosin in non-muscle cells induced by N-ethylmaleimide. *Exp. Cell Res.* **157:**95–115

Lawson, D. 1987. Distribution of myosin and relationship to active organization in cortical and subcortical areas of anti-body labelled, quick-frozen, deep-etched fibroblast cytoskeletons. *Cell Motil. Cytoskel.* **7:**368–380

Lewis, S.A., de Moura, J.L.C. 1982. Incorporation of cytoplasmic vesicles into apical membrane of mammalian urinary bladder epithelium. *Nature* **297:**685–688

Mills, J.W. 1987. The cell cytoskeleton: possible role in volume control. *Curr. Top. Memb. Trans.* **30:**75–101

Morris, C.E. 1992. Are stretch channels in molluscan cells and elsewhere physiological mechanotransducers? *Experientia* **48:**852–858

Morris, C.E., Horn, R. 1991. Failure to elicit neuronal macroscopic mechanosensitive currents anticipated by single channel studies. *Science* **251:**1246–1249

Morris, C.E., Moore, D. 1992. Efflux of $^{86}Rb^+$ from *Lymnaea* heart: effects of osmotic stress, depolarization, quinidine and 5-hydroxytryptamine. *Mol. Comp. Physiol.* **11:**192–198

Morris, C.E., Sigurdson, W.J. 1989. Stretch-inactivated ion channels coexist with stretch-activated ion channels. *Science* **243:**807–809

Morris, C.E., Williams, B., Sigurdson, W.J. 1989. Osmotically-induced volume changes in isolated cells of a pond snail. *Comp. Biochem. Physiol.* **92***A*:479–483

Reuzeau, C., Mills, L.R., Harris, J.A., Morris, C.E. 1994. Discrete and reversible vacuole-like dilations induced by osmomechanical perturbations of neurons. *J. Membrane Biol.* **145:**33–47

Ross, P.E., Garber, S.S., Cahalan, M.D. 1993. Membrane chloride conductance and capacitance in Jurkat T lymphocytes during osmotic swelling. *Biophys. J.* **66:**169–178

Schmidt, C.F., Svoboda, K., Lei, N., Petsche, I.B., Berman, L.E., Safinya, C.R., Grest, G.S. 1993. Existence of a flat phase in red cell membrane skeletons. *Science* **259:**952–955

Small, D.L., Morris, C.E. 1994. Delayed activation of single mechanosensitive channels in *Lymnaea* neurons. *Am J. Physiol.* **267:**C598–C606

Small, D.L., Morris, C.E. 1995. Pharmacology of stretch-activated K channels in *Lymnaea* neurons. *Br. J. Pharmacol.* **114:**180–186

Stoddard, J.S., Steinbach, J.H., Simchowitz, L. 1993. Whole cell $Cl^-$ currents in human neutrophils induced by cell swelling. *Am. J. Physiol.* **265:**C156–C165

Suleymanian, M.A., Baumgarten, C.M. 1994. Cardiac cell volume response to osmotic stress: temperature dependence and kinetics. *Biophys. J.* **66:***A*168

Sukhorukov, V.L., Arnold, W.M., Zimmermann, U. 1993. Hypotonically induced changes in the plasma membrane of cultured mammalian cells. *J. Membrane Biol.* **132:**27–40

Suzuki, A., Yamazaki, M., Ito, T. 1989. Osmoelastic coupling in biological structures: formation of parallel bundles of actin filaments in a crystalline-like structure caused by osmotic stress. *Biochem.* **28:**6513–6518

Wang, N., Butler, J.P., Ingber, D.E. 1993. Mechanotransduction across the cell surface and through the cytoskeleton. *Science* **260:**1124–1127

Watson, P.A. 1991. Function follows form: generation of intracellular signals by cell deformation. *FASEB J* **5:**2013–2019

Wilkerson, E.H., DiBona, D.R., Schafer, J.A. 1986. Analysis of structural changes during hypotonic swelling in Ehrlich ascites tumor cells. *Am. J. Physiol.* **251:**C104–C114

Wolfe, J., Dowgert, M.F., Steponkus, P.L. 1985. Dynamics of membrane exchange of the plasma membrane and the lysis of isolated protoplasts during rapid expansions in area. *J. Membrane Biol.* **86:**127–138